Inflammation
https://doi.org/10.1007/s10753-024-02117-z

CORRESPONDENCE

Arctiin Mitigates Neuronal Injury by Modulating the P2X7R/NLPR3 Inflammasome Signaling Pathway

Guang-Nan Jin[1] · Yu Wang[1] · Yi-Ming Liu[2] · Yu-Nan Lu[1] · Jing-Mei Lu[1] · Jing-He Wang[1] · Jing-Wen Ma[1] · Yan-Zhu Quan[1] · Hong-Yan Gao[1] · Yue-Xian Cui[2] · Xiang Xu[1] · Lian-Xun Piao[1]

Received: 21 May 2024 / Revised: 13 June 2024 / Accepted: 30 July 2024

Abstract

Depression, recognized globally as a primary cause of disability, has its pathogenesis closely related to neuroinflammation and neuronal damage. Arctiin (ARC), the major bioactive component of *Fructus arctii*, has various pharmacological activities, such as anti-inflammatory and neuroprotective effects. Building on previous findings that highlighted ARC's capability to mitigate depression by dampening microglial hyperactivation and thereby reducing neuroinflammatory responses and cortical neuronal damage in mice, the current study delves deeper into ARC's therapeutic potential by examining its impact on hippocampal neuronal damage in depression. Utilizing both chronic unpredictable mild stress (CUMS)-induced depression model in mice and corticosterone (CORT)-stimulated PC12 cell model of neuronal damage, the techniques including Nissl staining, immunohistochemistry, western blotting, ELISA, lactate dehydrogenase assays, colony formation assays, immunofluorescence staining and molecular docking were employed to unravel the mechanisms behind ARC's neuroprotective effects. The findings revealed that ARC not only mitigates hippocampal neuropathological damage and reduces serum CORT levels in CUMS-exposed mice but also enhances cell activity while reducing lactate dehydrogenase release in CORT-stimulated PC12 cells. ARC attenuated neuroinflammatory responses and neuronal apoptosis by inhibiting the overactivation of the P2X7 receptor (P2X7R)/NOD-like receptor family pyrin domain-containing 3 (NLRP3) inflammasome signaling pathway, similar to the effect of A438079 (P2X7R antagonist). Interestingly, pretreatment with A438079 blocked the neuroprotective effect of ARC. Computer modeling predicted that both ARC and A438079 have strong binding with P2X7R and they have the same binding site. These results suggested that ARC may exert a neuroprotective role by binding to P2X7R, thereby inhibiting the P2X7R/NLRP3 inflammasome signaling pathway.

KEY WORDS arctiin · depression · hippocampus · neuronal damage · neuroinflammation · P2X7R/NLRP3

Abbreviations

ARC	Arctiin
ASC	Apoptosis-associated speck-like protein containing a C-terminal caspase recruitment domain
CORT	Corticosterone
CUMS	Chronic unpredictable mild stress
DAPI	4′,6-Diamidino-2-phenylindole
DMSO	Dimethyl sulfoxide
ELISA	Enzyme-linked immunosorbent assay
IL-1β	Interleukin-1β
LDH	Lactate dehydrogenase
NLRP3	NOD-like receptor family pyrin domain containing 3
PBS	Phosphate-buffered saline
P2X7R	P2X7 receptor
TLR4	Toll-like receptor 4

Guang-Nan Jin, Yu Wang and Yi-Ming Liu contributed equally to this work.

✉ Yue-Xian Cui
24612923@qq.com

✉ Xiang Xu
xiangxu@ybu.edu.cn

✉ Lian-Xun Piao
lxpiao@ybu.edu.cn

[1] Key Laboratory of Natural Medicines of the Changbai Mountain, Ministry of Education, Molecular Medicine Research Center, College of Pharmacy, Yanbian University, Yanji 133002, Jilin Province, China

[2] Department of Neurology, Yanbian University Hospital, Yanbian University, Yanji 133000, Jilin Province, China

Published online: 17 August 2024

TNF-α Tumor necrosis factor-alpha
TNFR1 Tumor necrosis factor receptor 1

INTRODUCTION

Depression, a prevalent, chronic and recurrent mental illness, ranks as a leading cause of disability worldwide [1, 2]. According to the latest report of the World Health Organization, approximately 280 million people worldwide suffer from depression, with 800,000 people dying from depression every year [3]. The vast majority of clinically significant depressive episodes are triggered by objectively severe stressors [4]. The hippocampus is considered a critical stress-responsive brain region, changes in hippocampal volume, impaired neurogenesis and neuronal damage induced by stress and other negative stimuli contribute significantly to the onset and progression of depression [5, 6].

Stress-induced neuroinflammation has been shown to be closely related to the pathological process of depression [7–9]. Uncontrolled and sustained neuroinflammation disrupts hippocampal neuron function and exacerbates neuronal damage, affecting emotional and cognitive functions and leading to depression-like behaviors [10, 11]. Importantly, symptom remission in depressed patients often follows the normalization of inflammatory responses [11], highlighting the suppression of excessive neuroinflammatory responses as a pivotal strategy in treating depression.

The P2X7 receptor (P2X7R) belongs to the P2X subfamily of ligand-gated ion channel purinergic P2 receptors that can be activated by high concentrations of adenosine triphosphate and has been recognized as a potential target for therapeutic intervention in mental disorders [12, 13]. Moreover, the P2X7R has emerged as the most potent activator of the NOD-like receptor family pyrin domain containing 3 (NLRP3) inflammasome [14]. The activation of the NLRP3 inflammasome leads to the activation of caspase-1, which mediates the maturation and secretion of interleukin-1β (IL-1β) and the proinflammatory cytokine IL-18, thereby driving the inflammatory response that contributes to neuronal injury or death [15]. In animal models of stress-induced depression, consistent with studies of NLRP3-, P2X7R- and IL-1β-knockout strains, P2X7R or NLRP3 antagonist injections have demonstrated significant antidepressant and anti-inflammatory effects [16]. Currently, two P2X7R inhibitors (JNJ-54175446 and JNJ-55308942) undergoing phase II clinical trials for the treatment of major depression disorder [17, 18]. It is suggested that targeted inhibition of the P2X7R/NLRP3 inflammasome signaling pathway may have significant therapeutic potential in combating depression. At present, commonly used antidepressants in clinical practice include selective serotonin and norepinephrine reuptake inhibitors [19, 20]. However, many side effects, such as sexual dysfunction, hypertension and gastrointestinal reactions, limit the use of these antidepressants [21, 22]. Therefore, the search for safe and effective new antidepressant drugs is crucial. Natural compounds derived from medicinal plants have garnered significant attention as potential alternatives due to their low toxicity, fewer adverse effects and better compliance [22].

Arctiin (ARC) is the main active ingredient of *Fructus arctii* and exerts numerous pharmacological activities, such as anti-inflammatory and neuroprotective effects [23–25]. Lee et al. reported that ARC reversed scopolamine-induced cognitive deficits and increased brain cholinergic activity in mice [26]. Our previous study found that ARC protected against chronic unpredictable mild stress (CUMS)-induced cortical neuronal damage and ameliorated depressive-like behavior in mice by inhibiting high mobility group box 1/toll-like receptor 4 (TLR4) and tumor necrosis factor-alpha (TNF-α) /tumor necrosis factor receptor 1 (TNFR1) signaling cascades [27]. Recent studies have shown that excessive neuroinflammatory responses and neuronal damage in the hippocampus of CUMS or lipopolysaccharide-induced depression mice were associated with upregulation of TLR4 or P2X7R [28, 29]. However, the effects of ARC on hippocampal neuron damage in animal models of depression and its regulation on P2X7R-mediated signaling pathways in the hippocampus remain unclear. Therefore, we established an in vivo depression model with CUMS-induced C57BL/6 mice and an in vitro neuronal injury model with the corticosterone (CORT)-induced rat pheochromocytoma cell line PC12 cell to investigate the protective effect of ARC on hippocampal neuronal injury and its molecular mechanism.

MATERIALS AND METHODS

Reagents and Materials

PC12 cells were obtained from the American Type Culture Collection (Manassas, VA, USA). Roswell Park Memorial Institute 1640 medium and fetal bovine serum were purchased from Gibco (Grand Island, NY, USA). ARC was purchased from Shanghai YuanYe Biotechnology (Shanghai, China). CORT was purchased from MedChemExpress (Monmouth Junction, NJ, USA). Carboxymethyl cellulose sodium was obtained from Sangon Biotech (Shanghai, China). Dimethyl sulfoxide (DMSO) (purities greater than 98% according to high-performance liquid chromatography analysis) and crystal violet were purchased from Sigma-Aldrich (St. Louis, MO, USA). Lactate dehydrogenase (LDH) was purchased from Nanjing Jiancheng Bioengineering Institute (Nanjing, Jiangsu, China). Reagents and consumables related to apoptosis detection were purchased from Shanghai Biyuntian Biotechnology Co., Ltd. A438079, an

inhibitor of P2X7R, was purchased from MedChemExpress (Monmouth Junction, NJ, USA). Polyvinylidene difluoride membranes were obtained from Merck Millipore (Burlington, MA, USA). 4′,6-Diamidino-2-phenylindole (DAPI) was obtained from Roche Applied Science (10,236,276,001; Mannheim, Germany). All other chemicals were of reagent grade and obtained from Aladdin Industrial, Inc. (Shanghai, China).

Animals

Male C57BL/6 mice (18–22 g weight, 9 weeks old) were purchased from Liaoning Changsheng Biotechnology Co., Ltd. [SPF, SCXK (LIAO), Liaoning, China, 2015–001] and maintained under standard laboratory conditions with a 12 h light/dark cycle at 24 °C with free access to food and water. Mice were acclimatized to laboratory conditions for at least one week before the start of the experiment. All animal experiments were carried out according to the National Institutes of Health Guidelines for the Care and Use of Laboratory Animals (National Institutes of Health Publication No. 80–23, revised 1996) and approved by the Institutional Animal Care Committee of Yanbian University Medical School (resolution number: 201501022).

In Vitro Experimental Protocol

PC12 cells were cultured in Roswell Park Memorial Institute 1640 supplemented with 10% heat-inactivated fetal bovine serum, 1% penicillin (100 units/mL) and 1% streptomycin (100 units/mL) in an incubator at 37 °C and 5% CO_2. Subsequently, PC12 cells at the logarithmic growth stage were cultured in 96-well, 6-well or 24-well plates and 60-mm Petri dishes for 24 h. The cells were divided into six groups: the control group (uninduced and untreated), the vehicle group (400 μM CORT stimulation + 0.1% DMSO), the ARC group (400 μM CORT stimulation + 100 μM ARC), the ARC group (50 μM) (400 μM CORT stimulation + 50 μM ARC), the A438079 group (400 μM CORT stimulation + 10 μM A438079) and the ARC + A438079 group (400 μM CORT stimulation + 10 μM A438079 + 100 μM ARC, A438079 was added 1 h prior to ARC treatment). Finally, the cell supernatants and cell precipitates were collected and stored at -80 °C for subsequent experiments.

MTS Assay

PC12 cells were inoculated into 96-well plates (3.5×10^4 cells/well) and cultured in an incubator at 37 °C and 5% CO_2 for 24 h. The next day, the cells were treated with different concentrations of ARC (12.5, 25, 50, 100 and 200 μM) or CORT (50, 100, 200, 300 and 400 μM) for 36 h. All groups were treated with the same vehicle (0.1% DMSO). After 36 h, the cells were incubated with 20 μL of MTS [3-(4,5-dimethylthiazol-2-yl)-5-(3-carboxymethoxyphenyl)-2-(4-sulfophenyl)-2H-tet-razolium] solution (CellTiter 96® AQueous One Solution Reagent, Madison, WI, USA) for 2 h prior to the end of the culture. The optical density was determined at 490 nm with a Multiskan GO (Thermo Electron Corp., Marietta, OH, USA). The results are expressed as the percentage of viable cells relative to that of the controls (100% cell viability).

Viability of the CORT-Induced PC12 Cells

PC12 cells were seeded in 96-well plates (3.5×10^4 cells/well) and cultured for 24 h. The cells were then grouped and treated as described in in vitro experimental protocol. After 36 h, the cells were incubated with 20 μL of MTS as described in MTS assay.

LDH Assay

PC12 cells were cultured on 24-well plates (1.2×10^5 cells/well) and treated as described in in vitro experimental protocol. After 36 h, the media were collected, and the supernatants were separated by centrifugation at 2000 × g for 20 min at 4 °C. LDH in the culture supernatant was quantified using an LDH diagnostic kit (Jiancheng Institute of Biotechnology, Nanjing, China) in accordance with the manufacturer's instructions. The absorbance was measured at 450 nm using a Multiskan GO spectrophotometer.

$$\text{LDH activity (U/L)} = [\text{OD (sample hole)} - \text{OD (control hole)}] / [\text{OD (sample hole)} - \text{OD (blank hole)}] \times 200 \times \text{dilution multiple of sample.}$$

Colony Formation Assay

PC12 cells were seeded in 6-well plates (1×10^6 cells/well), incubated for 24 h, induced and treated as described in in vitro experimental protocol. After 5 days, the PC12 cells in the plates were washed three times with phosphate-buffered saline (PBS), fixed with 4% paraformaldehyde for 20 min and stained with crystal violet for 30 s. Six-well plates were washed with PBS, dried and photographed, and the number of colonies was counted using ImageJ (US National Institutes of Health, Bethesda, MD, USA; http://imagej.nih.gov/ij/, 1997–2012).

Immunofluorescence Staining

PC12 cells were cultured in 24-well plates with coverslips (1.2×10^5 cells/well) for 24 h and then induced and treated

as described in in vitro experimental protocol. After 36 h of treatment, the cells were fixed with precooled 100% methanol for 20 min, followed by permeation at room temperature with 0.2% Triton X-100 for 5 min. The cells were then incubated with PBS containing 5% bovine serum albumin for 1 h before incubation with rabbit anti-NLRP3 (1:250, Cat. No. PA579740, Invitrogen) and rabbit anti-Annexin V (1:200, Cat. No. ab14196, Abcam) at 4 °C overnight. The next day, the cells were incubated with Alexa Fluor® 594 donkey anti-rabbit IgG (H + L) (1:10, Cat. No. R37119, Thermo Fisher Scientific) to localize NLRP3 and Annexin V. The cells were stained with DAPI for 5 min before observation with an inverted fluorescence microscope (Olympus IX83, Tokyo, Japan). The mean fluorescence intensity of the NLRP3 and Annexin V-positive cells were determined by ImageJ software.

Animal Experiment Protocol

After 7 days of environmental adaptation, forty mice were randomly divided into four groups ($n = 10$): the control (not subjected to CUMS and treatment) group, vehicle [CUMS + 0.5% (w/v) carboxymethyl cellulose sodium] group, ARC (CUMS + 100 mg/kg body weight) group and ARC (CUMS + 50 mg/kg body weight) group. The mice were exposed to CUMS for 8 weeks, with drug administration via intragastric administration once daily during the final 4 weeks of the study. One hour after the last drug administration, all the mice were sacrificed via anesthetization. The hippocampus tissue and serum samples were collected and immediately frozen in liquid nitrogen for storage at -80 °C until use in subsequent experiments. The CUMS procedure is described in our previous study [27].

Serum CORT Assay

After all the experimental mice were sacrificed, blood samples were collected and separated by centrifugation at 900 × g for 10 min at 4 °C. The production of CORT in the serum was quantified using an enzyme-linked immunosorbent assay (ELISA) kit (MM-0061M1, Meimian, China) in accordance with the manufacturer's instructions.

Nissl Staining

The brain sections were cut into 8 μm sections with a freezing microtome. The slices were then stained with Nissl stain [1% cresyl violet (Xi'an Hat Biotechnology Co., Ltd., China)] solution at 50 °C and subsequently dehydrated through a graded alcohol series (70%, 80%, 90% and 100%). Then, the slices were cleaned with xylene and covered with a cover glass. Images were examined with an inverted fluorescence microscope and the number of Nissl-stained neurons was counted using ImageJ software.

Immunohistochemical Staining

The slices were fixed in methanol for 20 min, washed in PBS, and blocked with PBS containing 5% bovine serum albumin and 0.3% Triton X-100 for 1 h at room temperature. The slices were then incubated overnight at 4 °C with primary antibodies of rabbit anti-Annexin V (1:200, Cat. No. ab14196, Abcam) and mouse anti-NeuN (1:400, Cat. No. ab104224, Abcam). The next day, the sections were washed with PBS and subsequently incubated for 1 h at room temperature with Alexa Fluor 488 goat anti-mouse IgG (H + L) (1:500, Cat. No. ab150113, Abcam) to localize NeuN and Alexa Fluor 594 donkey anti-rabbit IgG (H + L) (1:10, Cat. No. R37119, Thermo Fisher Scientific) to localize Annexin V. The nuclei were stained with DAPI for 5 min and observed with the inverted fluorescence microscope. The proportions of Annexin V-positive neurons in the CA1, CA3 and DG regions of the hippocampus of CUMS-induced mice were determined using ImageJ software.

Western Blotting Analysis

The cell pellets or hippocampus tissue (20 mg) were lysed in 200 μL of RIPA lysis buffer containing 1% protease inhibitor (Solarbio, Beijing, China). The lysates were centrifuged, and the supernatants were collected. The protein concentration was determined by the bicinchoninic acid method. Equal amounts of protein were separated by sodium dodecyl sulfate–polyacrylamide gel electrophoresis and then transferred to polyvinylidene difluoride membranes. Subsequently, the membranes were blocked with 5% skim milk powder at room temperature for 1 h and incubated with primary antibodies specific for rabbit anti-P2X7R (1:1000, Cat. No. sc-514962, Santa Cruz), rabbit anti-NLRP3 (1:1000, Cat. No. PA5-79,740, Invitrogen), rabbit anti-apoptosis-associated speck-like protein containing a C-terminal caspase recruitment domain (ASC) (1:1000, Cat. No. ARG66211, Arigo Biolaboratories), rabbit anti-caspase 1 (1:1000, Cat. No. ARG57293, Arigo Biolaboratories), rabbit anti-IL-1β (1:1000; Cat. No. ab150777, Abcam), rabbit anti-mature IL-1β (1:1000, Cat. No. PA5-88,078, Invitrogen), rabbit anti-Bax (1:1000, Cat. No. PA5-78,857, Invitrogen), rabbit anti-Bcl-2 (1:1000, Cat. No. 7511, Bioworld) or rabbit anti-caspase 3 (1:1000, Cat. No.9662S, Cell Signaling Technology) at 4 °C overnight. Following further washing with 1 × PBS containing 0.05% Tween-20, the protein bands were incubated at room temperature for 1 h with the addition of a secondary horseradish peroxidase-conjugated goat anti-rabbit antibody (1:2000, Cat. No. SA00001-2, Proteintech).

Finally, the specific protein were detected by enhanced chemiluminescence (Millipore Co., Billerica, MA, USA). The β-actin serves as a loading control, which is quantified on the same blots as the protein of interest. After detecting the target protein, the membrane is subsequently stripped by SDS stripping buffer [30] and reprobed with the rabbit anti-β-actin (1:6000, Cat. No. 4967, Cell Signaling Technology). The density of the immunoreactive bands was analyzed using ImageJ software.

Molecular Docking

Molecular docking studies were performed to investigate the binding mode between the ARC or A438079 with Rattus norvegicus P2X7R using Autodock vina 1.1.2 [31]. The three-dimensional (3D) structure of the P2X7R (PDB ID: 6U9V) was downloaded from RCSB Protein Data Bank (http://www.rcsb.org). The 2D structure of the ARC and A438079 were drawn by ChemBioDraw Ultra 14.0 and were optimized by MM2 method using ChemBio3D Ultra 14.0 software to obtain the 3D structure. The AutoDockTools 1.5.6 package [32, 33] was employed to generate the docking input files. During the molecular docking study, the polar hydrogen atoms and Kollman united atom type charge were added to the protein. The search grid of the P2X7R was identified as center_x: 160.677, center_y: 170.652, and center_z: 226.319 with dimensions size_x: 15, size_y: 15, and size_z: 15. The value of exhaustiveness was set to 16. For Vina docking, the default parameters were used if it was not mentioned. The best-scoring pose as judged by the Vina docking score was chosen and visually analyzed using PyMoL 1.7.6 software (http://www.pymol.org).

Statistical Analysis

Statistical analyses were carried out using GraphPad Prism 8.0 (GraphPad Software Inc., San Diego, CA, USA). All the data were expressed as the mean ± SEM. The results were compared by one-way analysis of variance and Tukey's multiple comparison tests. $p < 0.05$ was considered to indicate a statistically significant difference between groups.

RESULTS

Effects of ARC on PC12 Cell Viability

To examine the effect of ARC on PC12 cell viability, PC12 cells were treated with various concentrations of ARC, and viability was evaluated using the MTS assay (Fig. 1). The

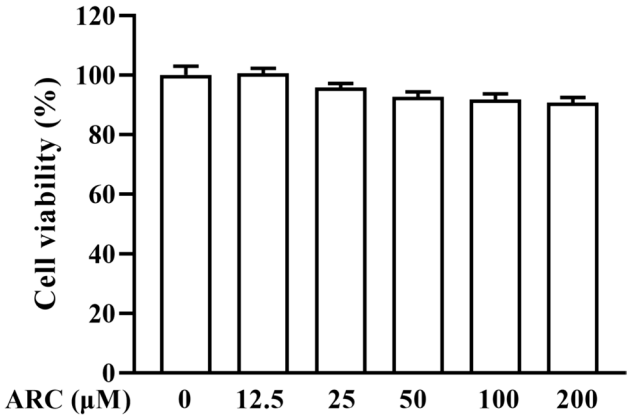

Fig. 1 The viability of PC12 cells. PC12 cells were treated with ARC (0–200 μM) for 36 h, after which cell viability was measured using the MTS assay. The data are expressed as the means ± SEM ($n = 6$).

MTS analysis revealed that ARC concentrations ranging from 12.5 μM to 200 μM did not exhibit significant cytotoxic effect on PC12 cells. Therefore, we chose concentrations of ARC (100 or 50 μM) for the subsequent experiments.

Protective Effect of ARC on CORT-Induced Cell Injury In Vitro

First, to assess the effect of CORT on cell viability, PC12 cells were exposed to various concentrations of CORT (0–400 μM). As illustrated in Fig. 2a, CORT decreased cell viability in a concentration-dependent manner, treatment with 400 μM CORT for 36 h resulted in a significant decline in cell viability compared to that of untreated cells ($p < 0.001$). Therefore, a concentration of 400 μM was used in subsequent experiments to induce the CORT-induced cell injury model.

Next, we determined the protective effects of ARC against CORT-induced PC12 cell injury. Treatment with ARC (100 or 50 μM) or A438079 (10 μM) alone significantly increased the viability of PC12 cells ($p < 0.05$ to $p < 0.01$ compared with vehicle group), while this effect was blocked by pretreatment with A438079 (P2X7R inhibitor) [$p < 0.01$ compared with ARC group (100 μM)] (Fig. 2b). As shown in Fig. 2c, LDH release was significantly elevated in PC12 cells treated with CORT for 36 h compared to the control group ($p < 0.001$). Treatment with ARC (100 or 50 μM) or A438079 (10 μM) significantly reduced LDH release compared with the vehicle group ($p < 0.001$), whereas the combined administration of ARC and A438079 failed to inhibit LDH release [$p < 0.05$ compared with the ARC group (100 μM)]. The colony formation assay further visually demonstrated the neuroprotective effect of ARC. The number of colonies in the vehicle group was significantly lower than

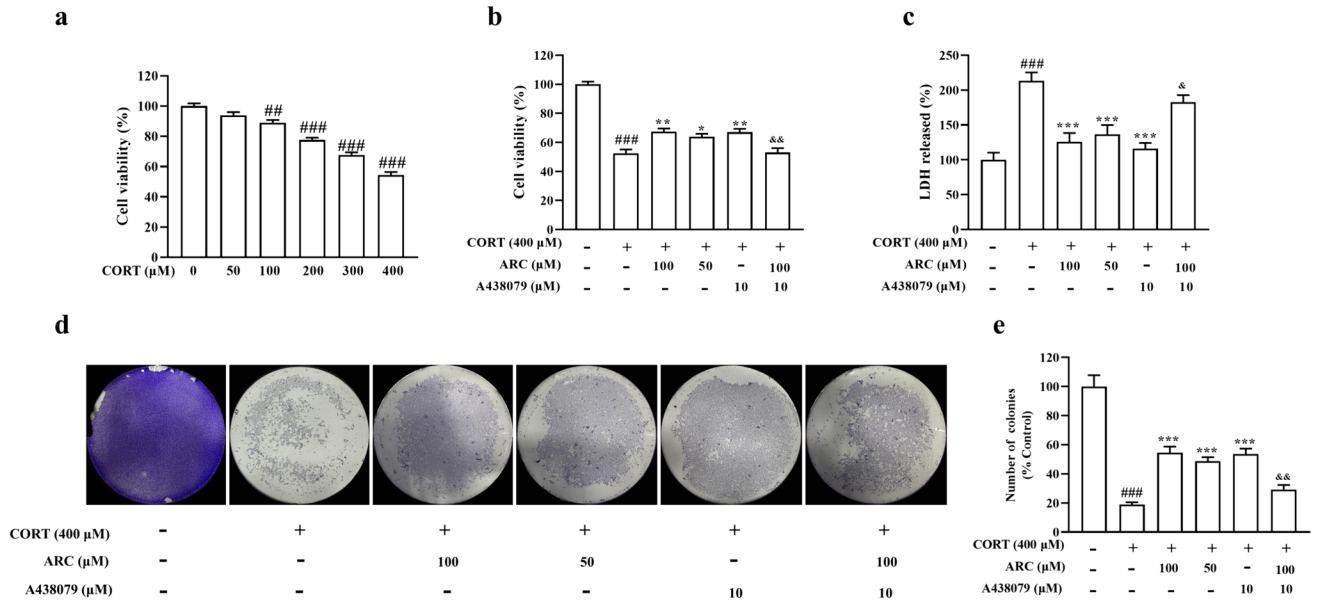

Fig. 2 Effect of ARC on CORT-induced damage in PC12 cells. **a** The cytotoxicity of CORT in PC12 cells. PC12 cells were treated with CORT (0–400 μM) for 36 h, and cell viability was measured by MTS. **b** The protective effect of ARC against CORT-induced damage in PC12 cells. PC12 cells were treated with CORT (400 μM) and the indicated concentrations of ARC for 36 h. A438079 (10 μM) was added 1 h prior to ARC (10 μM) treatment. Cell viability was determined by the MTS assay. **c** Effect of ARC on the LDH release rate from CORT-induced PC12 cells, as detected by LDH assays. **d** Photograph of a representative well from each group of colony formation assay. **e** The number of colonies was determined with ImageJ software. The data are expressed as the means ± SEM (a-c: $n=6$; d and e: $n=5$). $^{\#\#}p<0.01$, $^{\#\#\#}p<0.001$ vs. control group; $^{*}p<0.05$, $^{**}p<0.01$, $^{***}p<0.001$ vs. vehicle group; $^{\&}p<0.05$, $^{\&\&}p<0.01$ vs. ARC (100 μM) group.

that in the control group ($p<0.001$), and treatment with ARC and A438079 reversed this phenomenon ($p<0.001$ vs. vehicle group). However, the number of colonies in the A438079 + ARC group was significantly lower than that in the ARC group ($p<0.01$) (Fig. 2d and e). These results suggested that ARC or A438079 was protective against CORT stimulation-induced PC12 cell damage and pretreatment with A438079 reverses the protective effect of ARC.

Effects of ARC on CORT-Induced Cell Apoptosis In Vitro

Recent studies have shown that apoptosis may be the main manifestation of CORT stimulation-induced damage in PC12 cells and hippocampal cells [34]. Therefore, we detected the expressions of apoptosis-related protein in PC12 cells by western blotting analysis. As shown in Fig. 3a-c, ARC and A438079 treatment significantly increased the ratio of Bax to Bcl-2, cleaved-caspase 3 to pro-caspase 3 proteins expression ($p<0.001$ vs. vehicle group). In contrast to the results in the ARC group, A438079 + ARC treatment reversed the changes in the expression levels of these proteins [$p<0.001$ vs. ARC group (100 μM)].

In addition, we used immunofluorescence staining to detect the expression of Annexin V (an indicator of apoptosis) in CORT-stimulated PC12 cells (Fig. 3d and e). The Annexin V fluorescence intensity was significantly higher in the vehicle group than the control group ($p<0.001$). Treatment with either ARC or A438079 significantly reversed this effect ($p<0.001$ compared with the vehicle group), while there was no clear improvement in the A438079 + ARC group [$p<0.001$ vs. the ARC group (100 μM)]. The above results indicated that ARC and A438079 ameliorated CORT stimulation-induced PC12 cell apoptosis, while A438079 pretreatment blocked the anti-apoptotic effect of ARC.

Effects of ARC on the Activation of P2X7R/NLRP3 Signaling Pathway In Vitro

First, we analyzed the protein expressions of P2X7R and NLRP3 inflammasome-related protein in PC12 cells using western blotting and immunofluorescence staining. The expressions of P2X7R, NLRP3, ASC, cleaved-caspase 1/pro-caspase 1 and mature IL-1β/pro-IL-1β were significantly increased in PC12 cells stimulated with CORT ($p<0.001$ vs. control group, respectively) (Fig. 4a and b). However, ARC (100 or 50 μM) or A438079 (10 μM) treatment was significantly reduced above protein expressions ($p<0.05$ to $p<0.001$ vs. vehicle group, respectively). Immunofluorescence staining showed similar results (Fig. 4c and d), NLRP3 protein expression was elevated in the CORT-stimulated PC12 cells ($p<0.001$ vs. control

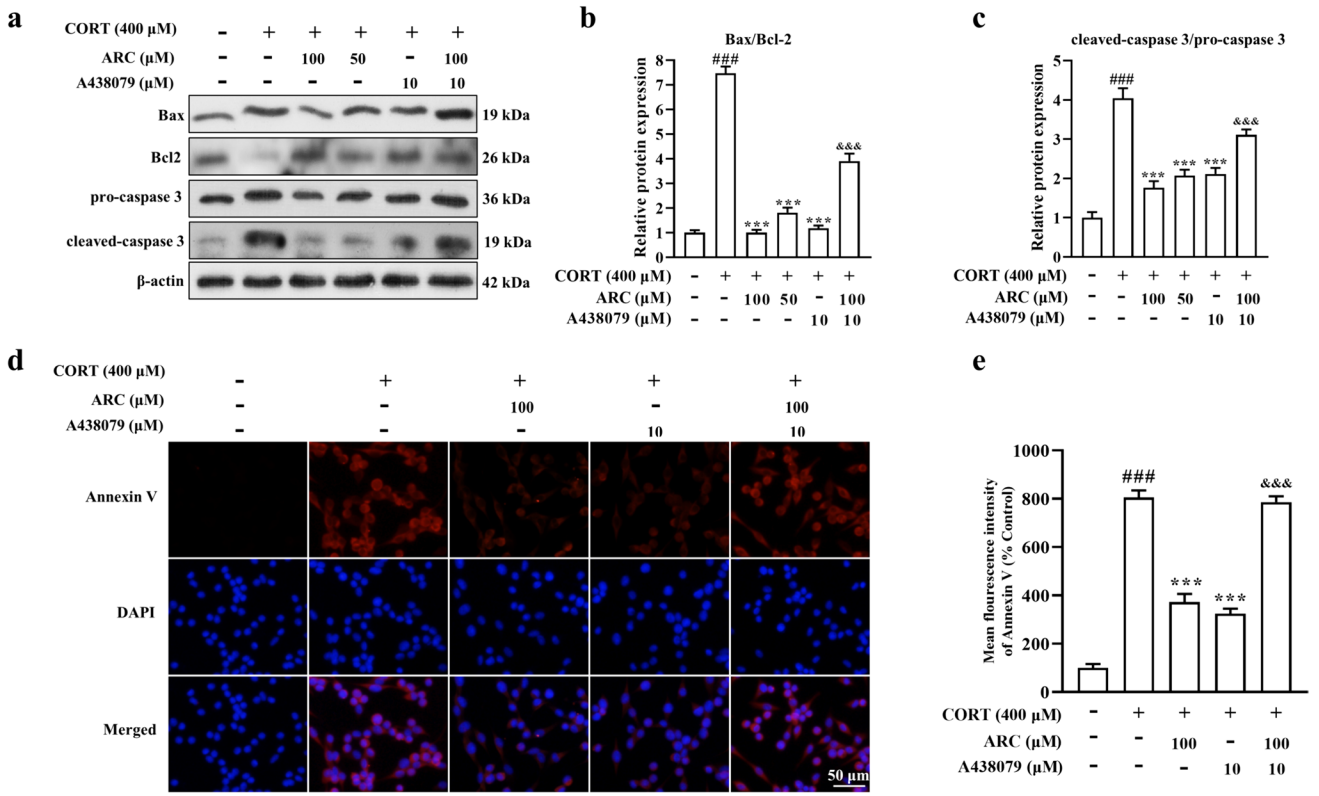

Fig. 3 Effect of ARC on the CORT-induced apoptosis of PC12 cells and related protein expressions. **a** Western blotting analysis of the expressions of apoptosis-related protein in PC12 cells. **b** Quantification of relative changes in Bax/Bcl-2 protein expression in PC12 cells. **c** The relative changes of cleaved-caspase 3/pro-caspase 3 protein expression in PC12 cells were quantitatively analyzed. **d** The expression of Annexin V (red) in PC12 cells was detected by immunofluorescence staining. **e** Quantitative analysis of the mean flourescence intensity of Annexin V. The data are expressed as the means ± SEM ($n = 5$). $^{###}p < 0.001$ vs. control group; $^{***}p < 0.001$ vs. vehicle group; $^{\&\&\&}p < 0.001$ vs. ARC (100 μM) group.

group), whereas ARC or A438079 treatment reversed this increase to a level comparable to that of the control ($p < 0.001$ vs. vehicle group). In addition, in the presence of A438079, ARC failed to inhibit P2X7R and NLRP3 inflammasome-related protein expressions [$p < 0.01$ to $p < 0.001$ compared with ARC group (100 μM)], it suggested that ARC and A438079 may compete with each other, thus inhibiting P2X7R.

To further elucidate the interaction between ARC or A438079 and the P2X7R, molecular docking techniques were utilized to determine the precise binding sites of ARC and A438079 on P2X7R. Both ARC and A438079 could adopt compact conformation to bind in the pocket of the P2X7R. In the P2X7R/ARC complex, ARC stretched into the hydrophobic pocket that consisted of A/Trp-167, A/Ala-296, C/Phe-88, C/Ala-91, C/Pro-96, C/Ala-296 and C/Ile-310, forming the strong hydrophobic bindings (Fig. 4e). Detailed analysis showed that one key hydrogen bond was observed between the ARC and the residue A/Tyr-298, with the bond length of 2.1 Å. In the P2X7R/A438079 complex, A438079 stretched into the hydrophobic pocket that consisted of A/Ala-296, B/Pro-96, C/Phe-93 and C/Ala-296, forming a strong hydrophobic binding (Fig. 4f). Importantly, a hydrogen bond was also found between A438079 and residue A/Tyr-298, with a bond length of 3.2 Å. This suggest that the combination of ARC and A438079 may affect ARC regulation of the P2X7R/NLRP3 signaling pathway by competing for the same binding site on P2X7R.

In summary, our study demonstrated that CORT induces P2X7R/NLRP3 inflammasome signaling pathway activation in PC12 cells, while treatment with ARC or A438079 inhibits this effect.

Effects of ARC on Serum Levels of CORT In Vivo

To determine the effects of stress and drug treatment on neuroendocrine activation, we assessed the serum CORT concentration in CUMS-induced mice. The serum CORT level was significantly higher in the CUMS group than control group ($p < 0.001$) (Fig. 5). Treatment with ARC

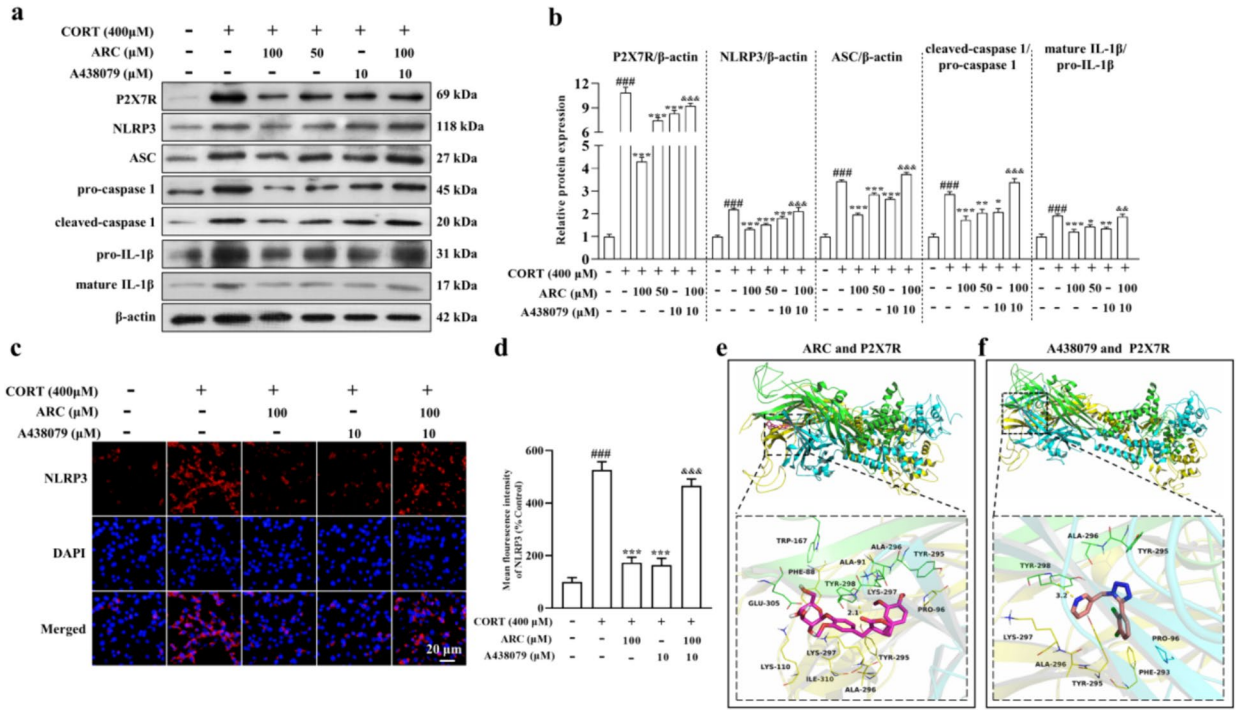

Fig. 4 The effects of ARC on the P2X7R/NLRP3 signaling pathway in CORT-induced PC12 cells. **a** Western blotting analysis of P2X7R/NLRP3-related protein expressions in PC12 cells. **b** Quantification of protein expression of P2X7R, NLRP3, ASC, cleaved-caspase 1/pro-caspase 1 and mature IL-1β/pro-IL-1β in PC12 cells. **c** The expression of NLRP3 (red) in PC12 cells was detected by immunofluorescence staining. Nuclei were stained with DAPI (blue). **d** Quantitative analysis for the mean fluorescence intensity of NLRP3. **e** Molecular docking results of ARC and P2X7R. **f** Molecular docking results of A438079 and P2X7R. The data are expressed as the means ± SEM (a-d: $n = 5$). $^{\#\#\#}p < 0.001$ vs. control group; $^{*}p < 0.05$, $^{**}p < 0.01$, $^{***}p < 0.001$ vs. vehicle group; $^{\&\&}p < 0.01$, $^{\&\&\&}p < 0.001$ vs. ARC (100 μM) group.

(100 or 50 mg/kg) significantly inhibited the CUMS-induced increase in CORT levels ($p < 0.05$ to $p < 0.01$ compared with vehicle group).

Protective Effects of ARC on CUMS-Induced Hippocampal Neuronal Damage In Vivo

To further reveal the neuroprotective effects of ARC, we conducted Nissl staining to observe the effect of ARC on morphological changes in the hippocampal neurons of CUMS-exposed mice. In the control group, hippocampal neurons displayed a rounded cytosol, distinct nuclei, and abundant Nissl vesicles. Conversely, neurons in the vehicle-treated group exhibited missing Nissl bodies, irregular arrangement, and poor stratification, accompanied by a significant reduction in the number of Nissl body neurons compared to the control group. These results suggested that chronic stress causes the dissolution and loss of Nissl bodies in hippocampal neurons and impairs neuronal structure and function. However, compared with vehicle treatment, ARC treatment significantly ameliorated the severity of CUMS-induced neuronal damage ($p < 0.01$ to $p < 0.001$) (Fig. 6a and b). Our results suggested that ARC has a protective effect against CUMS-induced neuronal damage in the mice hippocampus.

Effects of ARC on CUMS-Induced Hippocampal Neuronal Apoptosis In Vivo

We used double immunohistochemical staining to detect the expressions of Annexin V and NeuN (a specific neuronal marker) in hippocampal neurons. The number of Annexin V-positive neurons was significantly increased in the CA1, CA3 and DG regions of the mice in the vehicle group ($p < 0.001$ vs. control group). However, treatment with ARC significantly reduced the number of Annexin V-positive neurons in the hippocampus ($p < 0.001$) (Fig. 7a-d). In addition, we examined the expressions of apoptotic protein in the hippocampal tissues of CUMS mice using western blotting. Compared to the control group, CUMS induction reduced the ratio of Bax/Bcl-2 and cleaved-caspase 3/pro-caspase 3 protein expression ($p < 0.001$). This effect was reversed by ARC treatment ($p < 0.001$ compared with the vehicle group) (Fig. 7e-g), which was consistent with the double immunohistochemical staining results. These results suggested that

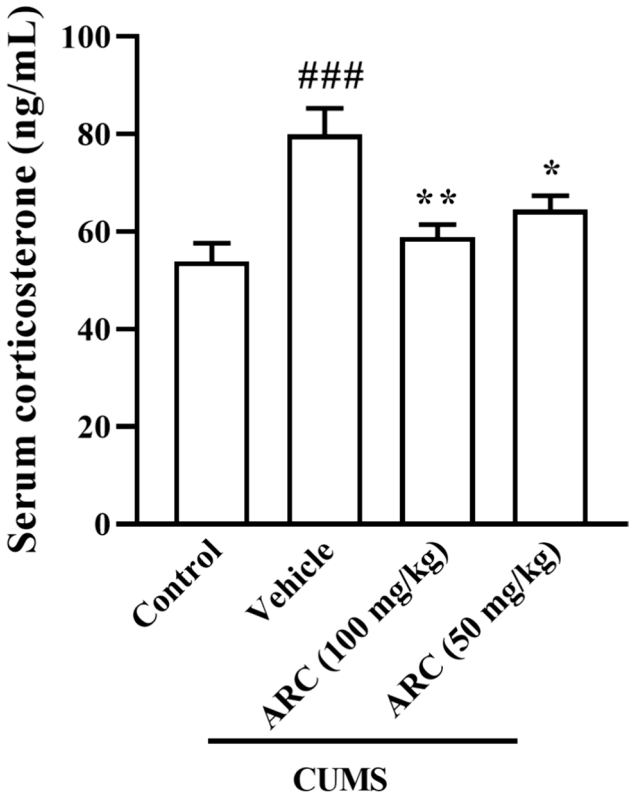

Fig. 5 Effect of ARC on serum CORT levels in CUMS-induced mice. Detection of CORT levels in the serum of CUMS-induced mice by ELISA. The data are expressed as the means ± SEM ($n = 5$). $^{###}p < 0.001$ vs. control group; $^{*}p < 0.05$, $^{**}p < 0.01$ vs. vehicle group.

ARC can effectively reduce neuronal apoptosis in the hippocampus of CUMS-induced mice.

Effects of ARC on the Activation of P2X7R/NLRP3 Signaling Pathway In Vivo

To further clarify the mechanism underlying the neuroprotective effects of ARC, we examined the expressions of protein related to the P2X7R/NLRP3 inflammasome signaling pathway in CUMS-induced mice hippocampal tissues by western blotting. Compared with control group, the protein expressions of P2X7R, NLRP3, ASC, cleaved-caspase 1/pro-caspase 1 and mature IL-1β/pro-IL-1β were significantly increased in vehicle group ($p < 0.01$ to $p < 0.001$) (Fig. 8a and b). However, the expression levels of these protein were downregulated by ARC (100 or 50 mg/kg) treatment ($p < 0.05$ to $p < 0.001$ compared with vehicle group). These results suggested that ARC inhibited CUMS-induced activation of the P2X7R/NLRP3 inflammasome signaling pathway in the mice hippocampus, which in turn attenuated the excessive inflammatory response.

DISCUSSION

As the main lignan compound isolated from the traditional Chinese medicine *Fructus arctii*, ARC has attracted the attention of researchers due to its various pharmacological activities, including anti-inflammatory, anti-infection

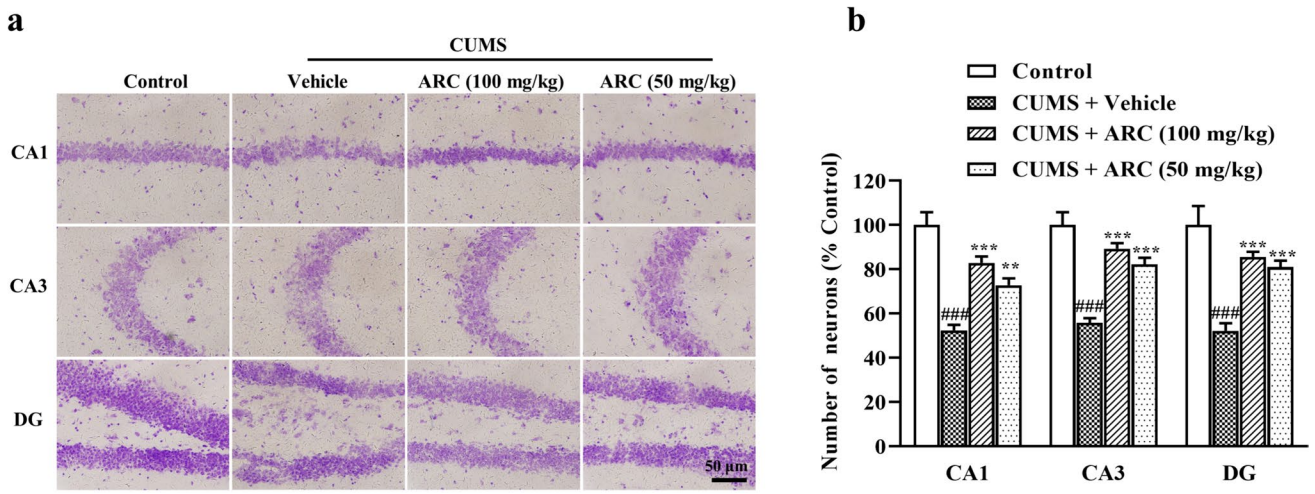

Fig. 6 Effects of ARC on neuronal damage in the hippocampal of CUMS-exposed mice. **a** Representative Nissl-stained sections of mouse hippocampal CA1, CA3 and DG regions. **b** Comparison of neuron numbers in the hippocampus CA1, CA3 and DG regions of mice. The data are expressed as the means ± SEM ($n = 5$). $^{###}p < 0.001$ vs. control group; $^{**}p < 0.01$, $^{***}p < 0.001$ vs. vehicle group.

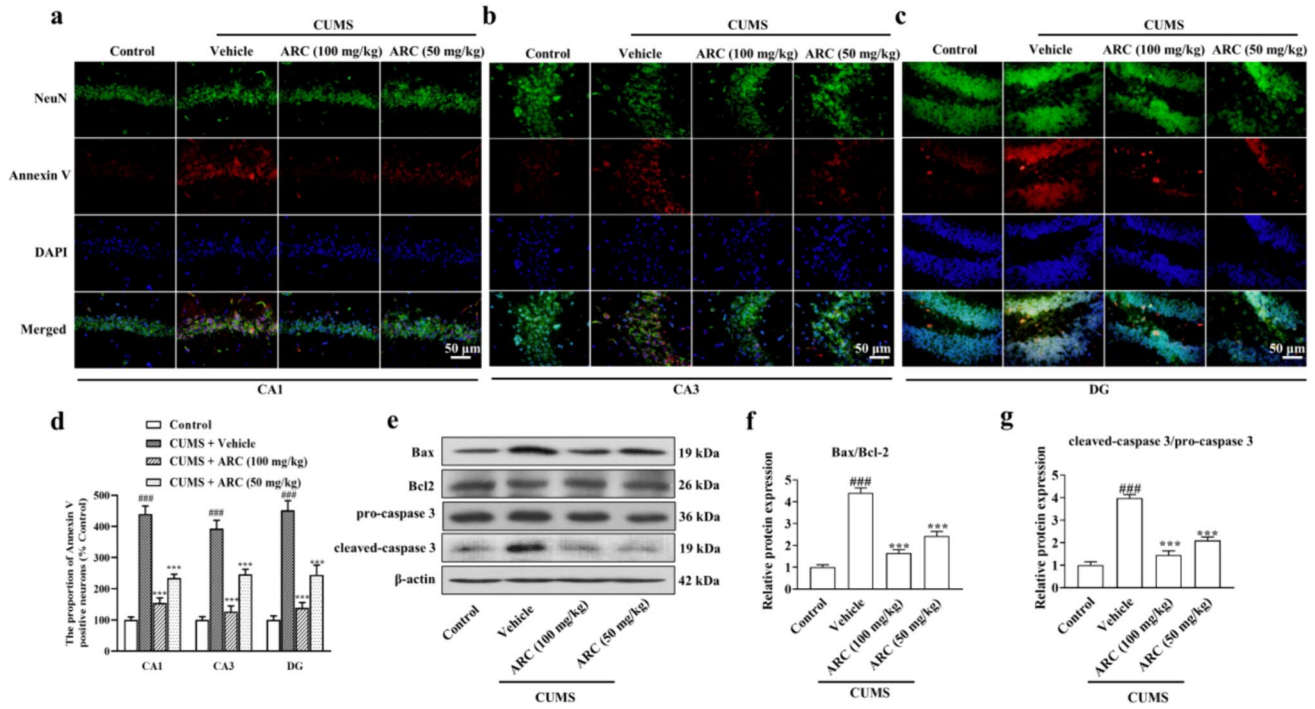

Fig. 7 Effect of ARC on hippocampal neuronal apoptosis in CUMS-exposed mice. **a-c** Double immunohistochemical staining for NeuN (green) and Annexin V (red) in the CA1 (**a**), CA3 (**b**) and DG (**c**) regions of the mice hippocampus. Nuclei were stained with DAPI (blue). **d** Quantitative analysis for the proportion of Annexin V positive neurons. **e** Western blotting analysis of the expressions of apoptosis-related protein in the mice hippocampus. **f** Quantification of relative changes in Bax/Bcl-2 protein expression in mice hippocampus. **g** The relative changes of cleaved-caspase 3/pro-caspase 3 protein expression in mice hippocampus were quantitatively analyzed. The data are expressed as the means ± SEM ($n = 5$). $^{###}p < 0.001$ vs. control group; $^{***}p < 0.001$ vs. vehicle group.

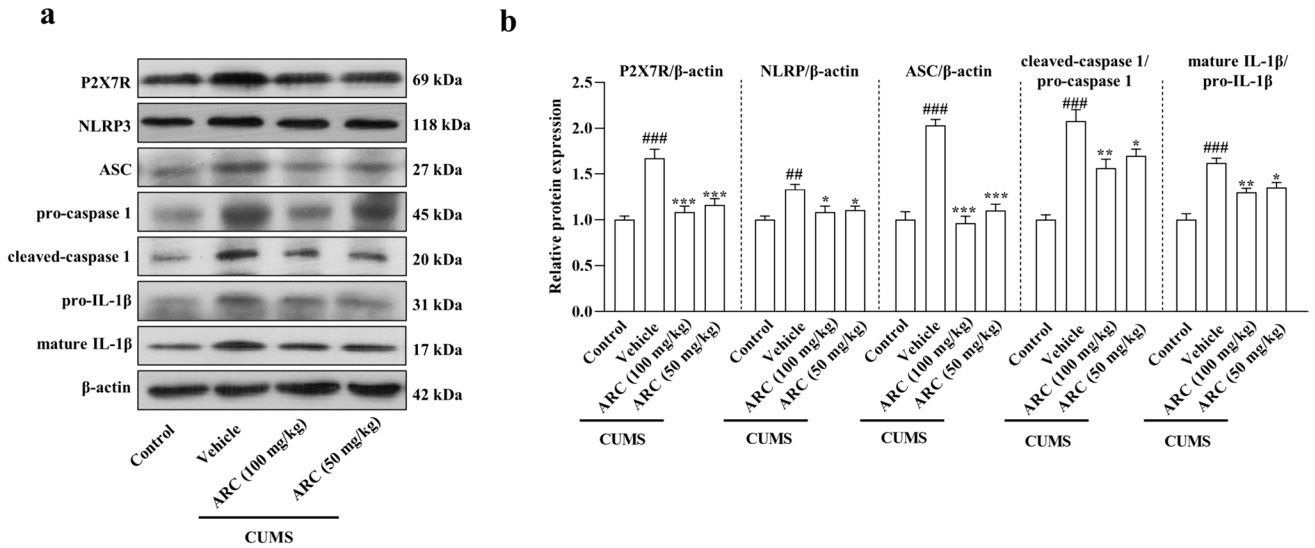

Fig. 8 The effects of ARC on the P2X7R/NLRP3 signaling pathway in vivo. **a** Western blotting analysis of P2X7R/NLRP3 inflammasome signaling pathway-related protein expressions in the hippocampus of mice. **b** The protein expression of P2X7R, NLRP3, ASC, cleaved-caspase 1/pro-caspase 1 and mature IL-1β/pro-IL-1β in mice hippocampus were quantitatively analyzed. The data are expressed as the means ± SEM ($n = 5$). $^{##}p < 0.01$, $^{###}p < 0.001$ vs. control group; $^{*}p < 0.05$, $^{**}p < 0.01$, $^{***}p < 0.001$ vs. vehicle group.

and neuroprotective effects [23, 25, 35]. Our previous study showed that ARC inhibited microglial hyperactivation-induced cortical neuronal damage through the high mobility group box 1/TLR4 and TNF-α/TNFR1 signaling pathways, thereby ameliorating depressive-like behaviors in CUMS-exposed mice [27]. In the present study, we shifted our focus to investigating the impact of ARC on hippocampal neuronal damage in an animal model of depression. We found that ARC ameliorated hippocampal neuronal injury and decreased serum levels of CORT in CUMS-exposed mice. In addition, ARC protected PC12 cells from the toxic effects of CORT by enhancing cell viability and suppressing cell apoptosis. ARC exerted a protective effect against hippocampal neuronal injury by attenuating excessive neuroinflammatory responses and neuronal apoptosis through the P2X7R/NLPR3 inflammasome signaling pathway.

Neuronal damage is one of the pathological features of many brain diseases, including depression [36, 37]. PC12 cells, renowned for their neuronal characteristics and high expression levels of glucocorticoid receptors [38], serve as a valuable in vitro model for studying neuronal damage induced by glucocorticoids such as CORT, a hallmark feature of depression [38–40]. Importantly, classical antidepressants such as venlafaxine [39] and fluoxetine [41] have been shown to have protective effects on the cytotoxicity of PC12 cells induced by high concentrations of CORT. Consistently, our study revealed that ARC increased cell viability and decreased LDH release, thereby ameliorating CORT stimulation-induced PC12 cell injury and exhibiting similar protective properties to those of conventional antidepressants.

The hippocampus, renowned for its pivotal roles in learning, memory and neuroendocrine regulation, stands as one of the most scrutinized brain regions in depression research [42, 43]. Severe and prolonged depression is usually accompanied by morphological changes in the brain, particularly a reduction in hippocampal volume and hippocampal atrophy [43]. Clinical investigations have consistently revealed diminished hippocampal neuronal cell size and density in individuals diagnosed with major depression compared to their non-depressed counterparts [44, 45]. Moreover, the hippocampus harbors numerous glucocorticoid receptors, and a surge in glucocorticoid levels in the stress response can lead to neuronal death or the failure of adult neurogenesis in the dentate gyrus, resulting in hippocampal damage [46, 47]. The CUMS model is commonly used in depression studies and induces behavioral and neurobiological changes in mice that are similar to human clinical depression [48]. Although previous studies have shown that 100 mg/kg ARC is the optimal dose to improve depression-like behavior induced by CUMS in mice [27], different from previous studies, this study focused on the protective effect of ARC on hippocampal neuron damage in mice, rather than cerebral cortex neurons. Therefore, it is necessary to re-evaluate the therapeutic effect of 50 mg/kg ARC. In the present study, we found that CORT levels were significantly elevated in the serum of CUMS-exposed mice, with substantial neuronal cell loss and atrophy in the CA1, CA3 and DG regions of the hippocampus. ARC treatment ameliorated this phenomenon in a dose-dependent manner, suggesting that ARC has a protective effect on hippocampal neuronal damage in CUMS-exposed mice. However, the underlying mechanisms of the protective effects of ARC on hippocampal neuronal damage are not fully understood.

Neuronal apoptosis is one of the main causes of depression-like phenotypes and is involved in hippocampal structural changes in the pathogenesis of depression-like behavior with different etiologies, such as diabetes-related depression and chronic stress depression [49, 50]. Both clinical and preclinical investigations have underscored a notable increase in neuronal apoptosis in individuals with depression, with antidepressants demonstrating efficacy in enhancing neuronal survival through apoptosis reduction [51, 52]. Our previous study demonstrated that sertraline, a frontline therapeutic agent in clinical practice, ameliorates depressive-like behavior in *Toxoplasma gondii*-infected mice by inhibiting neuronal cell apoptosis [53]. Therefore, the ability of drugs to inhibit neuronal apoptosis is closely related to their antidepressant effects. In the present study, we found that ARC significantly downregulated the ratio of Bax/Bcl-2 and cleaved-caspase 3/pro-caspase 3 protein expression in CUMS-exposed mice hippocampal tissues and CORT-stimulated PC12 cells. Moreover, ARC significantly ameliorated neuronal apoptosis in the CA1, CA3 and DG regions of the mice hippocampus and PC12 cell apoptosis, suggesting that ARC may exert neuroprotective effects by ameliorating apoptosis in hippocampal neurons.

Among purinergic receptors, P2X7R has received the most attention as a drug target for brain diseases, given its expression in regions of the human central nervous system, including the cerebral cortex, hippocampus and brainstem [54, 55]. Importantly, the *P2X7R* gene, located on chromosome 12q24.31, has been identified as a susceptibility locus for affective disorders, with P2X7R knockout exerting antidepressant-like effects in murine models [55]. In contrast, intrahippocampal injection of a P2X7R agonist markedly induced depressive-like behaviors in rats, consistent with the effect of CUMS exposure [56], suggesting a key role for P2X7R activation in the pathogenesis of depression. Clinical studies have reported elevated expressions of NLRP3 and caspase-1 genes in blood samples, along with increased serum levels of proinflammatory cytokines IL-1β and TNF-α in patients with depression [57]. Multiple animal model studies have shown that NLRP3 or caspase-1 inhibitor treatment reduces IL-1β protein levels in the serum and hippocampus and ameliorates CUMS-induced depressive-like behavior in mice [58]. The

above evidence suggests that the level of upregulation of the NLRP3/caspase-1/IL-1β signaling pathway is strongly associated with the severity of depression. Interestingly, NLRP3 inflammasome assembly, caspase-1 activation and IL-1β release are usually triggered by P2X7R activation, which to date is one of the most potent activators of the NLRP3 inflammasome [16, 59]. Recent investigations have demonstrated that neuroinflammation mediated by the P2X7R/NLRP3/IL-1β cascade plays a prominent role in the pathogenesis of various central nervous system disorders, such as migraine [60], ischemic brain injury [61] and Alzheimer's disease [62]. Moreover, our previous study revealed that excessive neuroinflammation downregulates the levels of the neurotransmitters dopamine and 5-hydroxytryptamine and promotes depressive-like behavior in mice [63–65]. Therefore, we hypothesize that P2X7R may induce excessive neuroinflammatory responses through activation of the NLRP3 inflammasome signaling pathway, which in turn induces the development of host depression-like behaviors.

Our previous studies have also demonstrated the strong binding affinity of ARC to both TLR4 and TNFR1, thereby modulating the TLR4- or TNFR1-mediated signaling pathway [27]. Interestingly, our recent investigation revealed that resveratrol and NLRP3-specific inhibitor (CY-09) compete for the same binding site on NLRP3, resulting in a synergistic effect of resveratrol and CY-09 in inhibiting the NLRP3 signaling pathway [66]. The findings from both in vitro and in vivo experiments in this study showed that ARC or A438079 (a specific P2X7R antagonist) significantly downregulated the expression of P2X7R and NLRP3 inflammasome signaling pathway-associated proteins, which in turn attenuated excessive neuroinflammation. However, upon pretreatment with A438079, the inhibitory effect of ARC on neuroinflammation induced by the P2X7R/NLRP3/IL-1β cascade disappeared. The molecular docking results showed that the binding affinity of ARC and A438079 to P2X7R is − 7.8 kcal/mol and − 7.1 kcal/mol, respectively. Interestingly, they share the same binding sites (A/Ala-296 and C/Ala-296), which extends into the hydrophobic pocket of P2X7R. Therefore, we hypothesized that ARC may effectively suppress the inflammatory response induced by P2X7R/NLRP3 signaling pathway through its interaction with P2X7R, similar to A438079. In addition to the P2X7R/NLRP3 inflammasome signaling pathway, inflammatory responses driven by the NLRP1 inflammasome have also been reported to be involved in chronic stress-induced depression-like behavior [67]. Consequently, further investigation is warranted to elucidate the role and interplay of P2X7R and other members of the NLR family in the pathogenesis of depression.

Increasing evidence indicates that P2X7R activation may lead to glutamate release and stimulation of neuroimmune responses, resulting in neuronal damage [68]. Díaz-Hernández et al. reported that primary cultured neurons expressing mutant huntingtin protein exhibit increased susceptibility to apoptosis

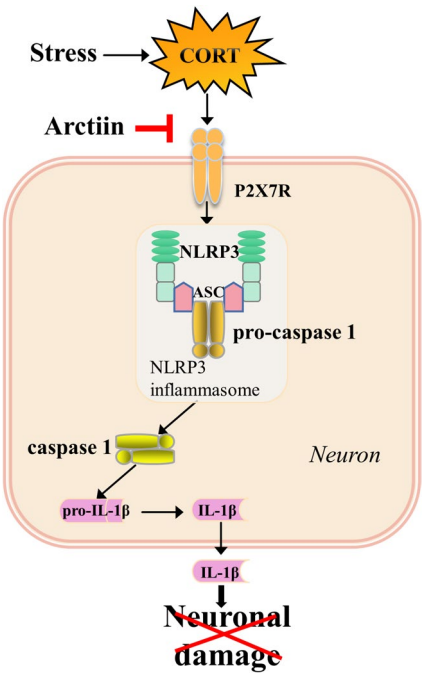

Fig. 9 Schematic representation of the mechanism of the protective effect of ARC on hippocampal neuronal damage in a stress-induced mice model of depression. ARC attenuates the excessive neuroinflammatory response induced by CUMS in the hippocampus of mice, thereby ameliorating hippocampal neuronal damage through modulating the activation of the P2X7R/NLRP3 inflammasome signaling pathway.

in response to P2X7R stimulation [69]. Importantly, P2X7R-dependent apoptosis has been shown to be closely associated with cell death in inflammatory diseases [70, 71]. P2X7R siRNA or P2X7R antagonist treatment significantly ameliorated neurological deficits and neuronal apoptosis in animal models of Huntington's disease [69], ischemic stroke [72] and hemorrhagic stroke [73]. In the present study, we found that the P2X7R inhibitor A438079 ameliorated CORT stimulation-induced cytotoxicity and apoptosis in PC12 cells, similar to the effects of ARC. Notably, A438079 pretreatment blocked the protective effect of ARC on PC12 cells, which may be related to the competition between A438079 and ARC for binding to the same site of P2X7R. It is suggested that P2X7R may act not only as a critical regulator of neuronal apoptosis in the hippocampus but also as a potential target through which ARC exerts neuroprotective effects.

Due to the complex biological mechanisms of depression and the adverse effects of synthetic or chemical drugs, plant-derived natural compounds offer a promising avenue for alternative medicinal interventions [74, 75]. The present study confirmed that ARC which extract from *Fructus arctii* ameliorated CUMS-induced neuronal damage in the hippocampus of mice through the P2X7R/NLRP3 inflammasome signaling pathway. However, we only used P2X7R

pharmacological inhibitor for exploring its potential mechanism study, and did not take the gene knockout or silencing method, which we will continue to investigate in the future.

CONCLUSION

Based on the insights from our preceding research that ARC ameliorated cerebral cortex damage and improved depression-like behaviors in CUMS-induced mice [27], the present study confirmed ARC exerts neuroprotective effect on hippocampal neuron injury. The underlying mechanism of this protective effect is illustrated in Fig. 9. ARC exerts an antidepressant effect by inhibiting the activation of the P2X7R/NLRP3 inflammasome signaling pathway, attenuating neuroinflammation and reducing apoptosis of hippocampal neurons. These findings provide a novel theoretical basis for understanding the pathogenesis of depression and highlight the potential utility of ARC as a lead compound in developing new treatments for depression.

Author Contribution GNJ contributed to investigation, data curation and writing—original draft. YW and YML contributed to investigation, data curation and writing. YNL, JML, JHW, JWM, YZQ and HYG contributed to investigation and data curation. YXC contributed to resources support. XX contributed to investigation, histopathology & formal analysis and writing—review & editing. LXP contributed to conceptualization, supervision, validation and writing—review & editing. All authors read and approved the final manuscript.

Funding This work was partially supported by the National Natural Science Foundation of China (81960375), the Jilin Provincial Science and Technology Department (YDZJ202201ZYTS294), Yanbian University Doctoral Research Fund Project (ydbq202218) and the Application Foundation Project of Yanbian University (ydkj202225).

Data Availability No datasets were generated or analysed during the current study.

Declarations

Ethics Approval and Consent to Participate All animal experiments were carried out according to the National Institutes of Health Guidelines for the Care and Use of Laboratory Animals (National Institutes of Health Publication No. 80–23, revised 1996) and approved by the Institutional Animal Care Committee of Yanbian University Medical School (resolution number: 201501022). All efforts were made to minimize suffering and the number of animals used during the studies.

Competing Interests The authors declare no competing interests.

References

1. McCarron, R. M., B. Shapiro, J. Rawles, and J. Luo. 2021. Depression. *Annals of Internal Medicine* 174 (5): ITC65–ITC80. https://doi.org/10.7326/AITC202105180.
2. Smith, K. 2014. Mental health: A world of depression. *Nature* 515 (7526): 181. https://doi.org/10.1038/515180a.
3. World Health Organization. 2023. Depression. https://www.who.int/zh/news-room/fact-sheets/detail/depression. Accessed 11 Dec 2023.
4. Hammen, C. 2018. Risk factors for depression: an autobiographical review. *Annual Review of Clinical Psychology* 14:1–28. https://doi.org/10.1146/annurev-clinpsy-050817-084811.
5. Li, X., T. Teng, W. Yan, L. Fan, X. Liu, G. Clarke, D. Zhu, Y. Jiang, Y. Xiang, Y. Yu, Y. Zhang, B. Yin, L. Lu, X. Zhou, and P. Xie. 2023. AKT and MAPK signaling pathways in hippocampus reveals the pathogenesis of depression in four stress-induced models. *Translational Psychiatry* 13 (1): 200. https://doi.org/10.1038/s41398-023-02486-3.
6. Liu, W., T. Ge, Y. Leng, Z. Pan, J. Fan, W. Yang, and R. Cui. 2017. The role of neural plasticity in depression: from hippocampus to prefrontal cortex. *Neural Plasticity* 2017:6871089. https://doi.org/10.1155/2017/6871089.
7. Jiang, H., X. Long, Y. Wang, X. Zhang, L. Chen, X. Yang, B. Zhao, Y. Zhang, Y. Chai, and T. Bao. 2024. Acupuncture ameliorates depression-like behaviors through modulating the neuroinflammation mediated by TLR4 signaling pathway in rats exposed to chronic restraint stress. *Molecular Neurobiology* 61 (5): 2606–2619. https://doi.org/10.1007/s12035-023-03737-6.
8. Medina-Rodriguez, E. M., A. A. Cruz, J. C. De Abreu, and E. Beurel. 2023. Stress, inflammation, microbiome and depression. *Pharmacology, Biochemistry, and Behavior* 227–228:173561. https://doi.org/10.1016/j.pbb.2023.173561.
9. Mehdi, S., S. U. D. Wani, K. L. Krishna, N. Kinattingal, and T. F. Roohi. 2023. A review on linking stress, depression, and insulin resistance via low-grade chronic inflammation. *Biochemistry and Biophysics Reports* 36:101571. https://doi.org/10.1016/j.bbrep.2023.101571.
10. Kim, Y. K., K. S. Na, A. M. Myint, and B. E. Leonard. 2016. The role of pro-inflammatory cytokines in neuroinflammation, neurogenesis and the neuroendocrine system in major depression. *Progress in Neuro-psychopharmacology & Biological Psychiatry* 64:277–284. https://doi.org/10.1016/j.pnpbp.2015.06.008.
11. Tao, W., K. Su, Y. Huang, Z. Lu, Y. Wang, L. Yang, G. Zhang, and W. Liu. 2023. Zuojinwan ameliorates CUMS-induced depressive-like behavior through inducing ubiquitination of MyD88 via SPOP/MyD88/NF-κB pathway. *Journal of Ethnopharmacology* 312:116487. https://doi.org/10.1016/j.jep.2023.116487.
12. Andrejew, R., Á. Oliveira-Giacomelli, D. E. Ribeiro, T. Glaser, V. F. Arnaud-Sampaio, C. Lameu, and H. Ulrich. 2020. The P2X7 receptor: central hub of brain diseases. *Frontiers in Molecular Neuroscience* 13:124. https://doi.org/10.3389/fnmol.2020.00124.
13. Ribeiro, D. E., A. L. Roncalho, T. Glaser, H. Ulrich, G. Wegener, and S. Joca. 2019. P2X7 receptor signaling in stress and depression. *International Journal of Molecular Sciences* 20 (11): 2778. https://doi.org/10.3390/ijms20112778.
14. Pelegrin, P. 2021. P2X7 receptor and the NLRP3 inflammasome: Partners in crime. *Biochemical Pharmacology* 187:114385. https://doi.org/10.1016/j.bcp.2020.114385.
15. Song, L., L. Pei, S. Yao, Y. Wu, and Y. Shang. 2017. NLRP3 Inflammasome in neurological diseases, from functions to therapies. *Frontiers in Cellular Neuroscience* 11:63. https://doi.org/10.3389/fncel.2017.00063.
16. von Muecke-Heim, I. A., C. Ries, L. Urbina, and J. M. Deussing. 2021. P2X7R antagonists in chronic stress-based depression models: A review. *European Archives of Psychiatry and Clinical Neuroscience* 271 (7): 1343–1358. https://doi.org/10.1007/s00406-021-01306-3.
17. Zhang, R., N. Li, M. Zhao, M. Tang, X. Jiang, X. Cai, N. Ye, K. Su, J. Peng, X. Zhang, W. Wu, and H. Ye. 2023. From lead to clinic: A review of the structural design of P2X7R antagonists.

European Journal of Medicinal Chemistry 251:115234. https://doi.org/10.1016/j.ejmech.2023.115234.
18. Lee, S., H. Ha, J. Jang, and Y. Byun. 2023. Recent advances in the development of antidepressants targeting the purinergic P2X7 receptor. *Current Medicinal Chemistry* 30 (2): 164–177. https://doi.org/10.2174/0929867329666220629141418.
19. Bonilla-Jaime, H., J. A. Sánchez-Salcedo, M. M. Estevez-Cabrera, T. Molina-Jiménez, J. L. Cortes-Altamirano, and A. Alfaro-Rodríguez. 2022. Depression and Pain: Use of Antidepressants. *Current Neuropharmacology* 20 (2): 384–402. https://doi.org/10.2174/1570159X19666210609161447.
20. Joshi, A. 2018. Selective serotonin re-uptake inhibitors: an overview. *Psychiatria Danubina* 30 (Suppl 7): 605–609.
21. Khawam, E. A., G. Laurencic, and D. A. Malone Jr. 2006. Side effects of antidepressants: an overview. *Cleveland Clinic Journal of Medicine* 73 (4): 351–361. https://doi.org/10.3949/ccjm.73.4.351.
22. Lin, R., L. Liu, M. Silva, J. Fang, Z. Zhou, H. Wang, J. Xu, T. Li, and W. Zheng. 2021. Hederagenin protects PC12 cells against corticosterone-induced injury by the activation of the PI3K/AKT pathway. *Frontiers in Pharmacology* 12:712876. https://doi.org/10.3389/fphar.2021.712876.
23. Du, Y., W. Li, Y. Li, J. Yang, X. Wang, S. Yin, X. Wang, O. I. Velez de-la-Paz, Y. Gao, H. Chen, X. Yin, and H. Shi. 2019. Repeated arctigenin treatment produces antidepressant- and anxiolytic-like effects in mice. *Brain Research Bulletin* 146:79–86. https://doi.org/10.1016/j.brainresbull.2018.12.005.
24. Zhou, B., G. Weng, Z. Huang, T. Liu, and F. Dai. 2018. Arctiin prevents LPS-induced acute lung injury via inhibition of PI3K/AKT signaling pathway in mice. *Inflammation* 41 (6): 2129–2135. https://doi.org/10.1007/s10753-018-0856-x.
25. Gao, Q., M. Yang, and Z. Zuo. 2018. Overview of the anti-inflammatory effects, pharmacokinetic properties and clinical efficacies of arctigenin and arctiin from Arctium lappa L. *Acta Pharmacologica Sinica* 39 (5): 787–801. https://doi.org/10.1038/aps.2018.32.
26. Lee, I. A., E. H. Joh, and D. H. Kim. 2011. Arctigenin isolated from the seeds of Arctium lappa ameliorates memory deficits in mice. *Planta Medica* 77 (13): 1525–1527. https://doi.org/10.1055/s-0030-1270746.
27. Xu, X., X. Y. Zeng, Y. X. Cui, Y. B. Li, J. H. Cheng, X. D. Zhao, G. H. Xu, J. Ma, H. N. Piao, X. Jin, and L. X. Piao. 2020. Antidepressive effect of arctiin by attenuating neuroinflammation via HMGB1/TLR4- and TNF-α/TNFR1-mediated NF-κB activation. *ACS Chemical Neuroscience* 11 (15): 2214–2230. https://doi.org/10.1021/acschemneuro.0c00120.
28. Li, J. M., T. Hu, C. L. Jiang, and W. Wang. 2022. Pinocembrin ameliorates depressive-like behaviors by regulating P2X7/TLR4 receptors expression in mouse hippocampus. *Behavioural Pharmacology* 33 (5): 301–308. https://doi.org/10.1097/FBP.0000000000000677.
29. Wang, C., C. Cui, X. Xie, B. Chen, L. Feng, and P. Jiang. 2024. Calcitriol attenuates lipopolysaccharide-induced neuroinflammation and depressive-like behaviors by suppressing the P2X7R/NLRP3/caspase-1 pathway. *Psychopharmacology (Berl)*. https://doi.org/10.1007/s00213-024-06565-1. Advance online publication.
30. Litovchick, L. 2020. Stripping of the immunoblot for reprobing. *Cold Spring Harbor Protocols* 2020 (3): 098491. https://doi.org/10.1101/pdb.prot098491.
31. Trott, O., and A. J. Olson. 2010. AutoDock Vina: Improving the speed and accuracy of docking with a new scoring function, efficient optimization, and multithreading. *Journal of Computational Chemistry* 31 (2): 455–461. https://doi.org/10.1002/jcc.21334.
32. Sanner, M. F. 1999. Python: A programming language for software integration and development. *Journal of Molecular Graphics & Modelling* 17 (1): 57–61.
33. Morris, G. M., R. Huey, W. Lindstrom, M. F. Sanner, R. K. Belew, D. S. Goodsell, and A. J. Olson. 2009. AutoDock4 and AutoDockTools4: Automated docking with selective receptor flexibility. *Journal of Computational Chemistry* 30 (16): 2785–2791. https://doi.org/10.1002/jcc.21256.
34. Yang, D., W. Wu, G. Gan, D. Wang, J. Gong, K. Fang, and F. Lu. 2020. (-)-Syringaresinol-4-O-β-D-glucopyranoside from Cortex Albizziae inhibits corticosterone-induced PC12 cell apoptosis and relieves the associated dysfunction. *Food and Chemical Toxicology* 141:111394. https://doi.org/10.1016/j.fct.2020.111394.
35. Lu, J. M., X. Xu, F. Aosai, M. Y. Zhang, L. L. Zhou, and L. X. Piao. 2024. Protective effect of arctiin against *Toxoplasma gondii* HSP70-induced allergic acute liver injury by disrupting the TLR4-mediated activation of cytosolic phospholipase A2 and platelet-activating factor. *International Immunopharmacology* 126:111254. https://doi.org/10.1016/j.intimp.2023.111254.
36. Komoltsev, I. G., and N. V. Gulyaeva. 2022. Brain trauma, glucocorticoids and neuroinflammation: dangerous liaisons for the hippocampus. *Biomedicines* 10 (5): 1139. https://doi.org/10.3390/biomedicines10051139.
37. Stephenson, J., E. Nutma, P. van der Valk, and S. Amor. 2018. Inflammation in CNS neurodegenerative diseases. *Immunology* 154 (2): 204–219. https://doi.org/10.1111/imm.12922.
38. Wang, H., X. Zhou, J. Huang, N. Mu, Z. Guo, Q. Wen, R. Wang, S. Chen, Z. P. Feng, and W. Zheng. 2013. The role of Akt/FoxO3a in the protective effect of venlafaxine against corticosterone-induced cell death in PC12 cells. *Psychopharmacology (Berl)* 228 (1): 129–141. https://doi.org/10.1007/s00213-013-3017-9.
39. Chai, Y., Y. Cai, Y. Fu, Y. Wang, Y. Zhang, X. Zhang, L. Zhu, M. Miao, and T. Yan. 2022. Salidroside ameliorates depression by suppressing NLRP3-Mediated pyroptosis via P2X7/NF-κB/NLRP3 signaling pathway. *Frontiers in Pharmacology* 13:812362. https://doi.org/10.3389/fphar.2022.812362.
40. Mao, Q. Q., Z. Huang, S. P. Ip, Y. F. Xian, and C. T. Che. 2012. Protective effects of piperine against corticosterone-induced neurotoxicity in PC12 cells. *Cellular and Molecular Neurobiology* 32 (4): 531–537. https://doi.org/10.1007/s10571-011-9786-y.
41. Zeng, B., Y. Li, B. Niu, X. Wang, Y. Cheng, Z. Zhou, T. You, Y. Liu, H. Wang, and J. Xu. 2016. Involvement of PI3K/Akt/FoxO3a and PKA/CREB signaling pathways in the protective effect of fluoxetine against corticosterone-induced cytotoxicity in PC12 cells. *Journal of Molecular Neuroscience:MN* 59 (4): 567–578. https://doi.org/10.1007/s12031-016-0779-7.
42. Gujral, S., H. Aizenstein, C. F. Reynolds 3rd., M. A. Butters, and K. I. Erickson. 2017. Exercise effects on depression: Possible neural mechanisms. *General Hospital Psychiatry* 49:2–10. https://doi.org/10.1016/j.genhosppsych.2017.04.012.
43. Lee, A. L., W. O. Ogle, and R. M. Sapolsky. 2002. Stress and depression: Possible links to neuron death in the hippocampus. *Bipolar Disorders* 4 (2): 117–128. https://doi.org/10.1034/j.1399-5618.2002.01144.x.
44. Kim, H. K., P. V. Nunes, K. C. Oliveira, L. T. Young, and B. Lafer. 2016. Neuropathological relationship between major depression and dementia: A hypothetical model and review. *Progress in Neuro-psychopharmacology & Biological Psychiatry* 67:51–57. https://doi.org/10.1016/j.pnpbp.2016.01.008.
45. O'Brien, J. T., A. Lloyd, I. McKeith, A. Gholkar, and N. Ferrier. 2004. A longitudinal study of hippocampal volume, cortisol levels, and cognition in older depressed subjects. *The American Journal of Psychiatry* 161 (11): 2081–2090. https://doi.org/10.1176/appi.ajp.161.11.2081.
46. Latt, H. M., H. Matsushita, M. Morino, Y. Koga, H. Michiue, T. Nishiki, K. Tomizawa, and H. Matsui. 2018. Oxytocin inhibits corticosterone-induced apoptosis in primary hippocampal neurons. *Neuroscience* 379:383–389. https://doi.org/10.1016/j.neuroscience.2018.03.025.

47. Tae, W. S., S. S. Kim, K. U. Lee, E. C. Nam, J. W. Choi, and J. I. Park. 2011. Hippocampal shape deformation in female patients with unremitting major depressive disorder. *AJNR. American Journal of Neuroradiology* 32 (4): 671–676. https://doi.org/10.3174/ajnr.A2367.
48. Yang, L., Y. Huang, F. Chen, Y. Wang, K. Su, M. Zhao, W. Tao, and W. Liu. 2023. Berberine attenuates depression-like behavior by modulating the hippocampal NLRP3 ubiquitination signaling pathway through Trim65. *International Immunopharmacology* 123:110808. https://doi.org/10.1016/j.intimp.2023.110808.
49. Shen, J., P. Zhang, Y. Li, C. Fan, T. Lan, W. Wang, and S. Y. Yu. 2021. Neuroprotective effects of microRNA-211-5p on chronic stress-induced neuronal apoptosis and depression-like behaviours. *Journal of Cellular and Molecular Medicine* 25 (14): 7028–7038. https://doi.org/10.1111/jcmm.16716.
50. Xu, D. H., J. K. Du, S. Y. Liu, H. Zhang, L. Yang, X. Y. Zhu, and Y. J. Liu. 2023. Upregulation of KLK8 contributes to CUMS-induced hippocampal neuronal apoptosis by cleaving NCAM1. *Cell Death & Disease* 14 (4): 278. https://doi.org/10.1038/s41419-023-05800-5.
51. Lucassen, P. J., E. Fuchs, and B. Czéh. 2004. Antidepressant treatment with tianeptine reduces apoptosis in the hippocampal dentate gyrus and temporal cortex. *Biological Psychiatry* 55 (8): 789–796. https://doi.org/10.1016/j.biopsych.2003.12.014.
52. Xu, L., J. Su, L. Guo, S. Wang, X. Deng, and S. Ma. 2019. Modulation of LPA1 receptor-mediated neuronal apoptosis by Saikosaponin-d: A target involved in depression. *Neuropharmacology* 155:150–161. https://doi.org/10.1016/j.neuropharm.2019.05.027.
53. Lan, H. W., Y. N. Lu, X. D. Zhao, G. N. Jin, J. M. Lu, C. H. Jin, J. Ma, X. Jin, X. Xu, and L. X. Piao. 2021. New role of sertraline against *Toxoplasma gondii*-induced depression-like behaviours in mice. *Parasite Immunology* 43 (12): e12893. https://doi.org/10.1111/pim.12893.
54. Gil, B., J. Smith, Y. Tang, P. Illes, and T. Engel. 2022. Beyond seizure control: treating comorbidities in epilepsy via targeting of the P2X7 receptor. *International Journal of Molecular Sciences* 23 (4): 2380. https://doi.org/10.3390/ijms23042380.
55. Huang, Z., and S. Tan. 2021. P2X7 receptor as a potential target for major depressive disorder. *Current Drug Targets* 22 (10): 1108–1120. https://doi.org/10.2174/1389450122666210120141908.
56. Yue, N., H. Huang, X. Zhu, Q. Han, Y. Wang, B. Li, Q. Liu, G. Wu, Y. Zhang, and J. Yu. 2017. Activation of P2X7 receptor and NLRP3 inflammasome assembly in hippocampal glial cells mediates chronic stress-induced depressive-like behaviors. *Journal of Neuroinflammation* 14 (1): 102. https://doi.org/10.1186/s12974-017-0865-y.
57. Alcocer-Gómez, E., M. de Miguel, N. Casas-Barquero, J. Núñez-Vasco, J. A. Sánchez-Alcazar, A. Fernández-Rodríguez, and M. D. Cordero. 2014. NLRP3 inflammasome is activated in mononuclear blood cells from patients with major depressive disorder. *Brain, Behavior, and Immunity* 36:111–117. https://doi.org/10.1016/j.bbi.2013.10.017.
58. Xia, C. Y., Y. X. Guo, W. W. Lian, Y. Yan, B. Z. Ma, Y. C. Cheng, J. K. Xu, J. He, and W. K. Zhang. 2023. The NLRP3 inflammasome in depression: Potential mechanisms and therapies. *Pharmacological Research* 187:106625. https://doi.org/10.1016/j.phrs.2022.106625.
59. Di Virgilio, F., D. Dal Ben, A. C. Sarti, A. L. Giuliani, and S. Falzoni. 2017. The P2X7 Receptor in infection and inflammation. *Immunity* 47 (1): 15–31. https://doi.org/10.1016/j.immuni.2017.06.020.
60. Wang, Y., Z. Shan, L. Zhang, S. Fan, Y. Zhou, L. Hu, Y. Wang, W. Li, and Z. Xiao. 2022. P2X7R/NLRP3 signaling pathway-mediated pyroptosis and neuroinflammation contributed to cognitive impairment in a mouse model of migraine. *The Journal of Headache and Pain* 23 (1): 75. https://doi.org/10.1186/s10194-022-01442-8.
61. Sun, K., J. Zhang, Q. Yang, J. Zhu, X. Zhang, K. Wu, Z. Li, W. Xie, and X. Luo. 2021. Dexmedetomidine exerts a protective effect on ischemic brain injury by inhibiting the P2X7R/NLRP3/Caspase-1 signaling pathway. *Brain Research Bulletin* 174:11–21. https://doi.org/10.1016/j.brainresbull.2021.05.006.
62. Islam, J., J. A. Cho, J. Y. Kim, K. S. Park, Y. J. Koh, C. Y. Chung, E. J. Lee, S. J. Nam, K. Lee, S. H. Kim, S. H. Park, D. Y. Lee, B. C. Kim, K. H. Lee, and S. Y. Seong. 2022. GPCR19 regulates P2X7R-Mediated NLRP3 inflammasomal activation of microglia by amyloid β in a mouse model of alzheimer's disease. *Frontiers in Immunology* 13:766919. https://doi.org/10.3389/fimmu.2022.766919.
63. Cheng, J. H., X. Xu, Y. B. Li, X. D. Zhao, F. Aosai, S. Y. Shi, C. H. Jin, J. S. Piao, J. Ma, H. N. Piao, X. J. Jin, and L. X. Piao. 2020. Arctigenin ameliorates depression-like behaviors in *Toxoplasma gondii*-infected intermediate hosts via the TLR4/NF-κB and TNFR1/NF-κB signaling pathways. *International Immunopharmacology* 82:106302. https://doi.org/10.1016/j.intimp.2020.106302.
64. Xu, X., H. N. Piao, F. Aosai, X. Y. Zeng, J. H. Cheng, Y. X. Cui, J. Li, J. Ma, H. R. Piao, X. Jin, and L. X. Piao. 2020. Arctigenin protects against depression by inhibiting microglial activation and neuroinflammation via HMGB1/TLR4/NF-κB and TNF-α/TNFR1/NF-κB pathways. *British Journal of Pharmacology* 177 (22): 5224–5245. https://doi.org/10.1111/bph.15261.
65. Xu, X., Y. N. Lu, J. H. Cheng, H. W. Lan, J. M. Lu, G. N. Jin, G. H. Xu, C. H. Jin, J. Ma, H. N. Piao, X. Jin, and L. X. Piao. 2022. Ginsenoside Rh2 reduces depression in offspring of mice with maternal toxoplasma infection during pregnancy by inhibiting microglial activation via the HMGB1/TLR4/NF-κB signaling pathway. *Journal of Ginseng Research* 46 (1): 62–70. https://doi.org/10.1016/j.jgr.2021.04.003.
66. Lu, Y. N., J. M. Lu, G. N. Jin, X. Y. Shen, J. H. Wang, J. W. Ma, Y. Wang, Y. M. Liu, Y. Z. Quan, H. Y. Gao, X. Xu, and L. X. Piao. 2024. A novel mechanism of resveratrol alleviates *Toxoplasma gondii* infection-induced pulmonary inflammation via inhibiting inflammasome activation. *Phytomedicine* 131:155765. https://doi.org/10.1016/j.phymed.2024.155765.
67. Song, A. Q., B. Gao, J. J. Fan, Y. J. Zhu, J. Zhou, Y. L. Wang, L. Z. Xu, and W. N. Wu. 2020. NLRP1 inflammasome contributes to chronic stress-induced depressive-like behaviors in mice. *Journal of Neuroinflammation* 17 (1): 178. https://doi.org/10.1186/s12974-020-01848-8.
68. Glaser, T., R. Andrejew, Á. Oliveira-Giacomelli, D. E. Ribeiro, L. Bonfim Marques, Q. Ye, W. J. Ren, A. Semyanov, P. Illes, Y. Tang, and H. Ulrich. 2020. Purinergic receptors in basal ganglia diseases: shared molecular mechanisms between huntington's and parkinson's disease. *Neuroscience Bulletin* 36 (11): 1299–1314. https://doi.org/10.1007/s12264-020-00582-8.
69. Díaz-Hernández, M., M. Díez-Zaera, J. Sánchez-Nogueiro, R. Gómez-Villafuertes, J. M. Canals, J. Alberch, M. T. Miras-Portugal, and J. J. Lucas. 2009. Altered P2X7-receptor level and function in mouse models of Huntington's disease and therapeutic efficacy of antagonist administration. *FASEB Journal* 23 (6): 1893–1906. https://doi.org/10.1096/fj.08-122275.
70. Kong, H., H. Zhao, H. Chen, Y. Song, and Y. Cui. 2022. Targeted P2X7/NLRP3 signaling pathway against inflammation, apoptosis, and pyroptosis of retinal endothelial cells in diabetic retinopathy. *Cell Death & Disease* 13 (4): 336. https://doi.org/10.1038/s41419-022-04786-w.
71. Li, Z., Z. Huang, and L. Bai. 2021. The P2X7 Receptor in Osteoarthritis. *Frontiers in Cell and Developmental Biology* 9:628330. https://doi.org/10.3389/fcell.2021.628330.

72. Ye, X., T. Shen, J. Hu, L. Zhang, Y. Zhang, L. Bao, C. Cui, G. Jin, K. Zan, Z. Zhang, X. Yang, H. Shi, J. Zu, M. Yu, C. Song, Y. Wang, S. Qi, and G. Cui. 2017. Purinergic 2X7 receptor/NLRP3 pathway triggers neuronal apoptosis after ischemic stroke in the mouse. *Experimental Neurology* 292:46–55. https://doi.org/10.1016/j.expneurol.2017.03.002.
73. Zhao, H., Y. Chen, and H. Feng. 2018. P2X7 Receptor-associated programmed cell death in the pathophysiology of hemorrhagic stroke. *Current Neuropharmacology* 16 (9): 1282–1295. https://doi.org/10.2174/1570159X16666180516094500.
74. Fathinezhad, Z., R. D. E. Sewell, Z. Lorigooini, and M. Rafieian-Kopaei. 2019. Depression and treatment with effective herbs. *Current Pharmaceutical Design* 25 (6): 738–745. https://doi.org/10.2174/1381612825666190402105803.
75. Wang, H., Y. He, Z. Sun, S. Ren, M. Liu, G. Wang, and J. Yang. 2022. Microglia in depression: An overview of microglia in the pathogenesis and treatment of depression. *Journal of Neuroinflammation* 19 (1): 132. https://doi.org/10.1186/s12974-022-02492-0.